

# Degradation and Transformation of Trichloroethylene in Miscible-Displacement Experiments through Zerovalent Metals

FRANCIS X. M. CASEY,<sup>†</sup>  
SAY KEE ONG,<sup>‡</sup> AND ROBERT HORTON<sup>\*†</sup>

Department of Agronomy and Department of Civil and  
Constructional Engineering, Iowa State University,  
Ames, Iowa 50011

Fate and transport of chlorinated solvents flowing through reactive barriers containing zerovalent metals are influenced by advection, dispersion, adsorption, and transformation reactions. Batch experiments or resident concentration column experiments have been used extensively to study reactions of zerovalent metals and for the design of in situ flow-through reactive barriers. However, extending results from batch or resident concentration column experiments to zerovalent metal flow-through systems may be challenging because sorption and degradation are indistinguishable, and nonequilibrium adsorption–desorption may occur. This study presents the first reported miscible-displacement experiments to study the fate and transport of chlorinated solvents flowing through zerovalent metals. The miscible-displacement experiments resulted in simultaneous breakthrough curves of trichloroethylene (TCE) and its reduction daughter product, ethylene. Pulses of dissolved TCE were introduced, at three different flow rates, into columns filled with sand, iron filings, or copper-plated iron filings (Cu–Fe). Column effluent was directed through a high performance liquid chromatography diode-array detector that determined concentrations of TCE and its degradation daughter products. Trichloroethylene did not degrade in the presence of sand. Slightly less TCE was observed with the Cu–Fe breakthrough curve than for the iron breakthrough curve. The simultaneous TCE and ethylene breakthrough curves were described with an equilibrium sorption/degradation model and a two-site partial nonequilibrium sorption model with degradation and production. Results of the experiments indicate that sorption is an important process to be considered when TCE is flowing through zerovalent metal systems.

## Introduction

Chlorinated solvents were the most commonly identified contaminants at nearly 300,000 to 400,000 hazardous waste sites in the United States as of 1994, and \$750 billion could be spent on their remediation over the next 30 years (1). Remediation methods that use zerovalent metals to degrade

chlorinated solvents have shown promise because they are relatively inexpensive, easy to maintain, and effectively eliminate trichloroethylene (TCE) and other chlorinated solvents. These remediation methods were pioneered by researchers at the Institute for Groundwater Research, University of Waterloo, Canada. Today, full-scale applications of zerovalent metals for the remediation of contaminated aquifers can be found at numerous locations including Belfast, Northern Ireland; Mountain View, CA; Cape Cod, MA; Coffeyville, KA; Elizabeth City, NC; Lakewood, CO; and New York, NY (2, 3).

The in situ applications of zerovalent metals utilize permeable reactive walls or aboveground columns through which contaminated groundwater flows. Flow-through remediation systems are designed to completely degrade chlorinated solvents and their daughter products as they pass out of the system. However, batch and resident concentration column experiments have been used extensively to study the reactions of zerovalent metals and to design remediation systems. These laboratory methods measure first-order degradation rate constants ( $k$ ) and usually do not take adsorption or the dynamics of a flowing system (i.e., advection and dispersion) into consideration (4). Resident concentration column experiments continuously introduce dissolved organic contaminant into columns filled with zerovalent metal, and resident concentrations are monitored at various sampling ports throughout the length of the column (1, 5–10). Resident concentration is the mass of solute per unit volume of fluid contained in an elementary volume of fluid at a given instant. To our knowledge, effluent concentrations have not been observed in any previously reported zerovalent metal column studies. For modeling purposes, if proper concentration or flux boundary conditions are not described, difficulties involving dispersion may arise, and it becomes difficult to predict effluent concentrations from resident concentrations (11)—this may compromise the design of flow-through remediation systems. Furthermore, if the zerovalent material is not homogeneous there may be increased difficulties in predicting effluent concentrations from resident concentrations. With regards to an aboveground pilot-scale field column demonstration, Gillham et al. (8) stated that “the performance did not meet expectations based on the results of the initial laboratory tests”. It may be that the “unmet expectations” resulted from the use of batch and resident concentration column experiments that may be associated with difficulties when extending the results to zerovalent metal flow-through remediation systems.

The objective of this research was to use miscible-displacement breakthrough curves, in conjunction with mathematical model description, to study the fate and transport of TCE flowing through zerovalent metals. Influent pulses of TCE were passed through three different porous media (sand, iron, or iron-plated copper [Cu–Fe]) at three different steady-state flow rates. Breakthrough curves were described with convective-dispersive models to identify the processes that govern the fate and transport of TCE flowing through zerovalent metals.

## Materials and Methods

**Miscible-Displacement System.** A schematic of the system used for the miscible-displacement experiments is presented in Figure 1. The system was comprised of two portions: (1) a column transport portion and (2) an analytical portion. Casey et al. (12) provided in-depth description and evaluation of this system. This system was unique because it was fully

\* Corresponding author phone: (515)294-7843; fax: (515)294-3163; e-mail: rhorton@iastate.edu.

<sup>†</sup> Department of Agronomy.

<sup>‡</sup> Department of Civil and Constructional Engineering.

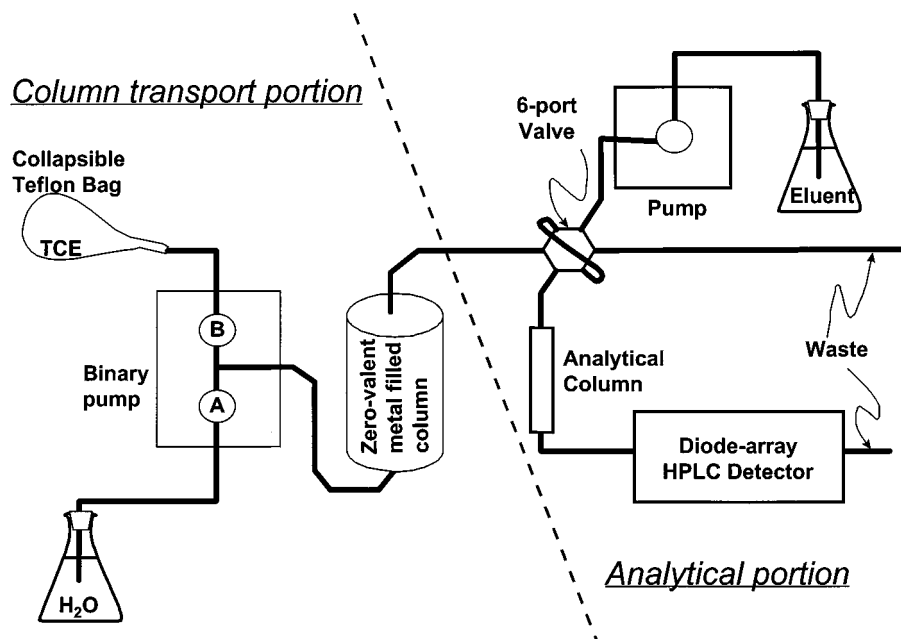


FIGURE 1. Schematic of system used for miscible-displacement experiments. The system consists of two portions: a transport portion and an analytical portion.

enclosed and constructed of nonsorbing material resulting in minimum chemical loss due to volatility or sorption. Also, this system could simultaneously detect multiple chemicals present in the column effluent. The column transport portion consisted of a fully programmable binary pump with one reservoir supplied by a Teflon bag (6) filled with 92 mg L<sup>-1</sup> TCE and the other reservoir supplied by degassed Nanopure water. Gas was purged from the Nanopure water by boiling and placing the boiled water under vacuum as it cooled. The flow rate and the supply ratio from each pump's reservoir was programmed, so that concentrations up to 96 mg L<sup>-1</sup> could be achieved. The column transport portion was connected to the analytical portion by a six-port, two-way, automated valve with a 50- $\mu$ L sampling loop. The analytical portion of the system was a basic high performance liquid chromatography (HPLC) setup. A 50- $\mu$ L effluent sample could be diverted to the analytical portion of the system when the six-port valve was switched. A direct injection port was also used to determine known solution concentrations and develop chemical calibrations.

For the calibration curves, standards for TCE and probable daughter products such as 1,1-dichloroethylene; 1,2-cis-dichloroethylene; 1,2-trans-dichloroethylene; vinyl chloride; and ethylene were prepared. Separation of TCE and its daughter products was achieved using an eluent of 88% acetonitrile and 12% water and a flow rate of 1 mL min<sup>-1</sup>. An Alltech C-18 analytical column was used, and the peak detection wavelength was 212 nm. The concentration detection limit for each chemical was nearly 0.01 mg L<sup>-1</sup>.

Effluent samples were fraction-collected in 10-mL glass syringes with a Swage-lok fitting for copper (Cu) analysis. Analysis for free Cu<sup>2+</sup> was done using a Cu<sup>2+</sup>-ion-selective electrode (Orion 94-29), a reference electrode (Orion 900200), and a pH/ion meter (Corning 135). The detection limit for Cu<sup>2+</sup> was within the order of magnitude of 10<sup>-7</sup> M. Furthermore, at the end of each run, the pH of the column effluent and the influent water was measured using a pH/ion meter (Corning 135).

**Column Packing Materials.** Three stainless steel columns (21.4 mm diameter and 124 mm length) were packed with Ottawa sand, 40-mesh iron filings (Fisher Scientific), or 40-mesh Fisher iron filings plated with 1.78% Cu. Placed at each column end were distribution plates, wire mesh, and a 2- $\mu$ m

frit, all made of stainless steel. Stainless steel was used because it is relatively inert and does not reduce TCE (13). The distribution plates and wire mesh assured flow uniformity and distribution through the column, while the frits prevented large particles from leaving the column.

The sand was washed with deionized water and dried before it was packed into the column. The column bulk density ( $\rho_b$ ) was 1.40 mg m<sup>-3</sup>. Assuming a particle density ( $\rho_s$ ) of 2.63 mg m<sup>-3</sup> the column porosity was calculated to be 0.47.

Degassed Nanopure water was then used to slowly saturate (flow rate = 0.2 mL min<sup>-1</sup>) the column from the bottom up while vacuum was applied to the top. Once water appeared at the top of the column, it was capped while water was still pumped into the bottom of the column. The water pumped into the bottom pressurized the column above  $1.03 \times 10^7$  Pa and forced any entrapped gas into the water. The column pressure was then released and flushed with more degassed water. This was repeated until nearly 100  $\pm$  0.2% saturation was achieved.

Before the iron filings were packed into the column, they were acid-washed to remove impurities by soaking in a 5 vol % solution of sulfuric acid in Nanopure water for 15 min. Aliquots of ethanol and Nanopure water were then used to rinse the iron, and then the iron was oven-dried at 35–40 °C overnight. Specific surface measurements were obtained from two  $\pm$ 10-g samples using BET nitrogen sorption isotherms (14). The mean specific surface for the two samples was 5.76 m<sup>2</sup> g<sup>-1</sup>. The  $\rho_s$  was 6.4 Mg m<sup>-3</sup> measured with a bath pycnometer. The column was packed so that the surface area concentration (15) was 21,147 m<sup>2</sup> L<sup>-1</sup>. Using the previously described method to saturate the sand column, nearly 100  $\pm$  0.7% saturation was achieved with the iron column.

Copper was plated onto the iron filings by a cold electroless method, where the substrate metal acts as a reducing agent to displace Cu ions from solution and coat the surface (16). Iron was added to a solution of copper sulfate. The mean specific surface obtained from the BET nitrogen sorption isotherms for two  $\pm$ 10-g Cu-Fe samples was 3.73 m<sup>2</sup> g<sup>-1</sup>, the pycnometer-measured value of  $\rho_s$  was 7.1 Mg m<sup>-3</sup>, and the packed column surface area concentration was 22,417 m<sup>2</sup>

L<sup>-1</sup>. The previously described saturation technique was used to achieve nearly 100 ± 0.5% saturation for the Cu–Fe column.

**Transport Experiments.** A series of three different steady-state flow miscible-displacement experiments were done on each porous media. The three different flow rates used resulted in respective pore water velocities (*v*) of 12.4, 6.2, or 3.1 mm min<sup>-1</sup>, so that one pore volume was displaced each 10, 20, or 40 min. Although the velocities fell in the range of observed groundwater flow, they were somewhat high. If the velocities were slower there may not have been any observable concentrations in the effluent due to TCE reduction. The column retention times were varied, while the sorption sites remained constant. Varying the retention times and using the same column were done to distinguish between degradation and adsorption. For each experiment a pulse of 46 mg L<sup>-1</sup> TCE was introduced into the column for one pore volume and then flushed out. Column effluent was sampled every 5 min for analysis with the online HPLC, and the effluent was monitored for at least 10 pore volumes. The order in which the column experiments were done was fast, intermediate, and then slow flow rate; after which a replicate of the first fast flow rate was done for the iron and Cu–Fe columns. The columns were flushed with at least 40 pore volumes of Nanopure water between each experiment.

A nonsorbing anionic tracer, Cl<sup>-</sup>, was used to determine whether the zerovalent metal columns displayed physical nonequilibrium (17). A uniform background solution of 0.0025 M of KCl was applied to the columns, and then one pore volume of 0.1 M KCl was applied. Water was passed through these columns so that one pore volume was displaced every 26 min. Effluent was fraction-collected and analyzed with a Haache Buchler Digital Chloridometer.

**Mathematical Models.** The program CXTFIT version 2.0 (18) was used to estimate the dispersion (*D*) coefficients for the Cl<sup>-</sup> breakthrough curves of the zerovalent metal columns and for the TCE breakthrough curves of the sand column. The measured breakthrough curve data were fitted with the analytical solution to the one-dimensional, discrete, advective-dispersion equation using least-squares parameter optimization. The optimized *D* values from the column breakthrough curves were used to estimate column dispersivity ( $\lambda = D/v$ ) (19).

The model HYDRUS-1D version 2.0 (20) was used to describe the zerovalent metal breakthrough curve experiments. This model was used in the forward mode with specified model parameters to predict the experimental breakthrough curves. It was also used to curve-fit experimental breakthrough curves by optimizing parameters so that the model solution fit the measured data. A subroutine within HYDRUS-1D numerically solved advective-dispersive transport of the solutes involved in the sequential decay and production reactions for up to four chain members. However, HYDRUS-1D could only be used to fit the first chemical in the series when optimizing parameters. The following set of coupled differential equations shows the one-dimensional, advective-dispersive transport of the four chain members under steady-state flow and linear equilibrium transport conditions (21):

$$R_1 \frac{\partial C_1}{\partial t} = D \frac{\partial^2 C_1}{\partial x^2} - v \frac{\partial C_1}{\partial x} - k_{s,1} \frac{\rho_b K_{d,1}}{\theta} C_1 \quad (1a)$$

$$R_i \frac{\partial C_i}{\partial t} = D \frac{\partial^2 C_i}{\partial x^2} - v \frac{\partial C_i}{\partial x} - k_{s,i} \frac{\rho_b K_{d,i}}{\theta} C_i + k_{s,i-1} \frac{\rho_b K_{d,i-1}}{\theta} C_{i-1}, \quad (i = 2, 3, 4) \quad (1b)$$

where *C<sub>i</sub>* are solute concentrations, *x* is the distance, *t* is the time, *k<sub>s,i</sub>* are first-order degradation rate constants, and the

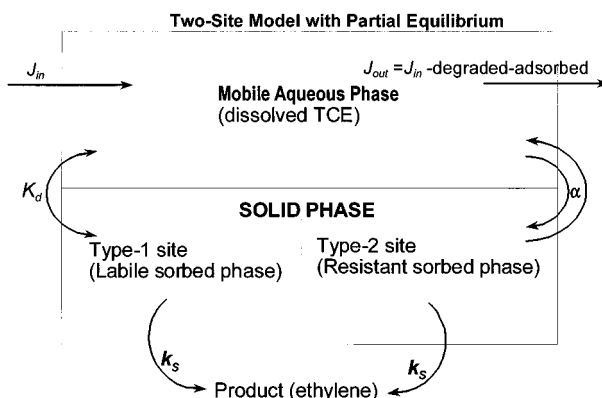


FIGURE 2. Schematic of two-site advective-dispersive model with partial equilibrium and partial kinetic sorption and degradation. Where *J* is the solute flux density, *K<sub>d</sub>* is partitioning coefficient, and  $\alpha$  is the first-order adsorption rate coefficient. Double-headed arrows link compartments that reach equilibrium instantaneously.

retardation factors (*R<sub>i</sub>*) are given by

$$R_i = 1 + \frac{\rho_b K_{d,i}}{\theta} \quad (2)$$

where *K<sub>d,i</sub>* are empirical distribution coefficients, and  $\theta$  is the volumetric water content; the subscript *i* denotes the *i*th chain member. Equations 1a, 1b, and 2 are the equilibrium sorption with first-order degradation rate model.

The concept of two-site sorption nonequilibrium adsorption-desorption reactions (22, 23) was also considered for the zerovalent metal breakthrough curves and it was implemented in HYDRUS-1D. Sorption on labile exchange sites or Type-1 sites (*S<sub>1</sub>*) was assumed to be instantaneous, while on remaining resistant exchange sites or Type-2 sites (*S<sub>2</sub>*) the sorption was considered kinetic (Figure 2). The degradation was considered to be a surface process, and the equation that governs mass transport for the system as a whole under steady-state flow and in a uniform system follows

$$\left(1 + \frac{\rho_b f K_{d,1}}{\theta}\right) \frac{\partial C_1}{\partial t} = D \frac{\partial^2 C_1}{\partial x^2} - v \frac{\partial C_1}{\partial x} - \frac{\alpha_1 \rho_b}{\theta} [(1-f) K_{d,1} C_1 - S_{2,1}] - k_{s,1} \frac{f \rho_b K_{d,1}}{\theta} C_1 \quad (3a)$$

$$\left(1 + \frac{\rho_b f K_{d,i}}{\theta}\right) \frac{\partial C_i}{\partial t} = D \frac{\partial^2 C_i}{\partial x^2} - v \frac{\partial C_i}{\partial x} - \frac{\alpha_i \rho_b}{\theta} [(1-f) K_{d,i} C_i - S_{2,i}] - k_{s,i} \frac{f \rho_b K_{d,i}}{\theta} C_i - k_{s,2} S_{2,i} + k_{s,i-1} \frac{f \rho_b K_{d,i-1}}{\theta} C_{i-1} + k_{s,i-1} S_{2,i-1} \quad (i = 2, 3, 4) \quad (3b)$$

where *f* is the fraction of exchange sites assumed to be at equilibrium, *k<sub>s,i</sub>* are rate constants for first-order degradation rate of the sorbed phase, and  $\alpha_i$  are first-order kinetic rate sorption constants.

## Results and Discussion

**TCE Transport in Sand Column.** Only TCE was detected in the effluent breakthrough curves for the sand columns (Figure 3), and no degradation daughter products were measured. The mass of the TCE applied to the system relative to the mass of TCE recovered in the effluent ranged from 98% to 102%. These results suggest that there was no degradation of TCE in the presence of sand or stainless steel. Similarly, Gillham and O'Hannesin (13) found no detectable degradation of TCE in the presence of stainless steel. The mass balance calculations were subjected to numerical and detection errors

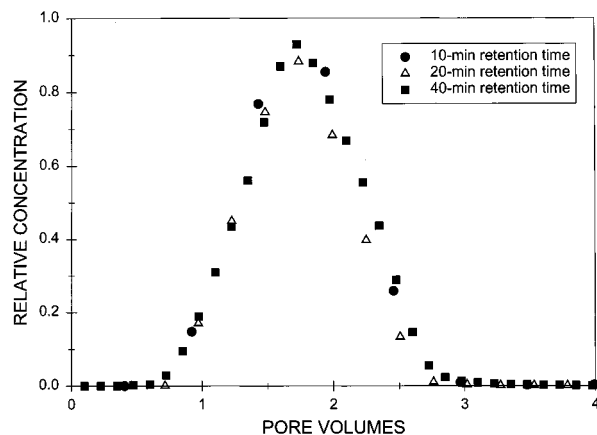


FIGURE 3. Trichloroethylene breakthrough curves through sand column. The input pulse was one pore volume for each experiment.

that may have caused TCE mass recovery values slightly greater or less than 100%.

**TCE Transport in Zerovalent Metal Columns.** Ethylene and TCE were the only compounds detected in the effluent of all iron column (Figures 4) and Cu-Fe column (Figures 5) breakthrough curves. For the iron column, 74%, 87%, and 95% of the TCE was reduced for the flow rate series of fast, intermediate, and slow, respectively. For the Cu-Fe column, 79%, 89%, and 98% of the TCE was reduced, respectively, for this flow rate series. These results suggested that the Cu-Fe column slightly reduced more TCE at each flow rate than did the iron column; however, since these differences only ranged between 2% to 5%, then they could have also been caused by numerical integration and/or detection errors. Several studies have noted that the presence of a second metal increased the reduction rates of the zerovalent iron (i.e., 8, 10, 16, 24, 25). Although a secondary metal such as nickel and Cu enhances TCE degradation and decreases the amount of reduction daughter products, there remains a danger of producing metal plumes in the groundwater (3). However, no Cu was detected in the Cu-Fe column effluent, which supported using Cu-Fe as a remediation media. For the series of flow rates, the mass of carbon present in the effluent (in the form of TCE and ethylene) relative to the mass of carbon introduced into the column (in the form of TCE) was 96%, 97%, and 94% for the iron column and 100%, 89%, and 82% for the Cu-Fe column. The lower carbon mass balance for the Cu-Fe column may reflect the reduction of ethylene to other aliphatic compounds such as ethane and butene, which were not analyzed by the HPLC. This may explain why the carbon mass balance decreased as column retention times within the Cu-Fe column increased. For both iron or Cu-Fe columns, the last replicate breakthrough curve was very similar to the first fast flow breakthrough curve (Figures 4 and 5). The similarity of these breakthrough curves indicated that there was no significant change in degradation capacity of the iron column or Cu-Fe column between each experiment.

Gillham and O'Hannesin (6), Orth and Gillham (7), and Gotpagar et al. (26) suggested that TCE reduction was a surface process where the TCE molecule does not leave the iron surface until sufficient electrons have been transferred for complete dechlorination. This may explain why there were no degradation daughter products detected in the column effluent for all experiments, since the TCE would remain attached to the iron surface until ethylene was formed. The attachment of TCE to the iron surface may reflect its hydrophobicity or a covalent bonding induced by the transfer of the first electron in the reduction process (7). The TCE dechlorination product, ethylene, would have to dissociate from the surface site before that site was available for further

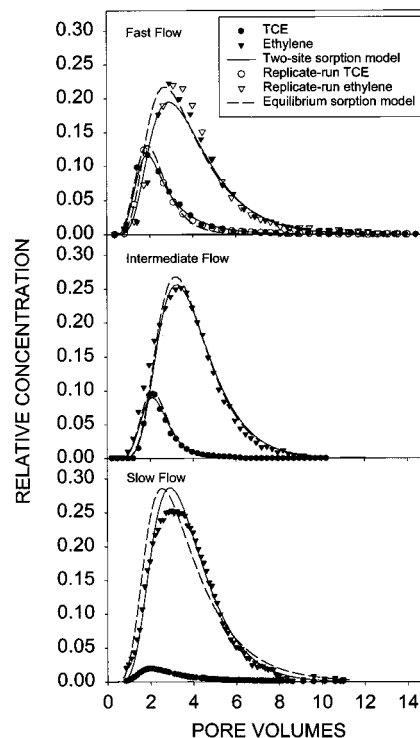


FIGURE 4. Iron column TCE breakthrough curves for fast, intermediate, and slow flow rates. The input pulse was one pore volume for each experiment. The equilibrium and two-site sorption models were fitted to the TCE breakthrough curves.

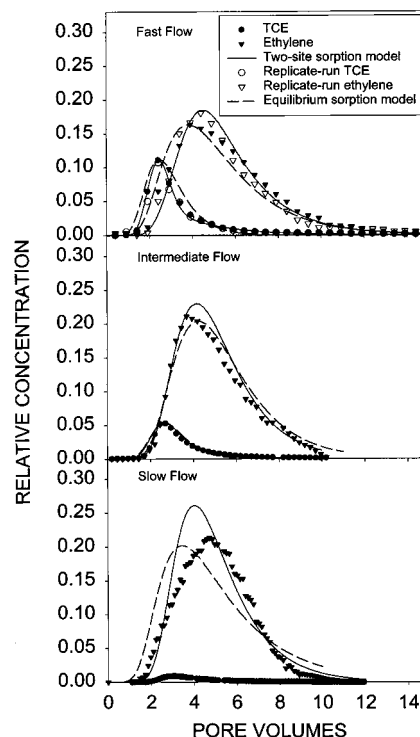


FIGURE 5. Copper-iron column TCE breakthrough curves for fast, intermediate, and slow flow rates. The input pulse was one pore volume for each experiment. The equilibrium and two-site sorption models were fitted to the TCE breakthrough curves.

reaction with the reactant solute molecules, TCE (4). As a result, individual molecules of TCE would bypass reactive sorption sites that were occupied and they would exit the column intact. This was further indicated by the increased mass of TCE degraded and increased production of ethylene

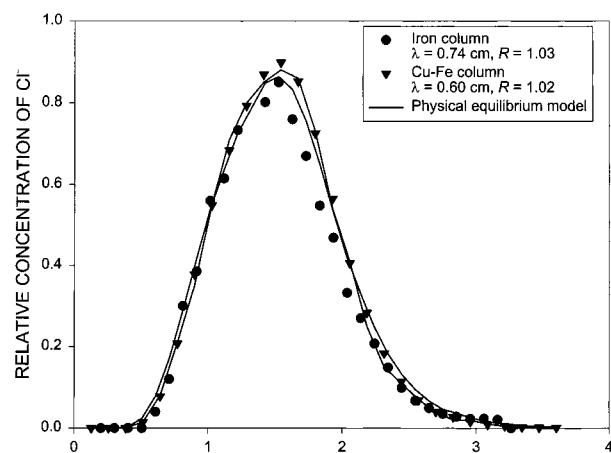
**TABLE 1. Values of Equilibrium Sorption Model (Eqs 1a and 1b) and Two-Site Sorption Model (Eqs 3a and 3b) Parameters with 95% CI for the Fitted Parameters<sup>a</sup>**

flow rate/column	equilibrium sorption model				
	$\lambda$ (cm)	$K_d$ (L Kg <sup>-1</sup> )	$k_{s,sa}$ (Lh <sup>-1</sup> m <sup>-2</sup> ) × 10 <sup>-5</sup>		
fast/iron	0.97 (±1.11)	0.40 (±0.44)	19 (±11.0)		
inter./iron	1.03 (±0.18)	0.40 (±0.04)	21 (±1.5)		
slow/iron	3.00 (±1.97)	1.36 (±0.75)	8.9 (±2.0)		
fast/Cu-Fe	1.61 (±0.62)	0.46 (±0.07)	18 (±1.8)		
inter./Cu-Fe	1.08 (±0.43)	0.498 (±0.08)	14 (±1.3)		
slow/Cu-Fe	3.75 (±2.50)	1.77 (±0.94)	6 (±0.79)		

flow rate/column	two-site sorption model				
	$\lambda$ (cm)	$K_d$ (L Kg <sup>-1</sup> )	$f$	$\alpha$ (h <sup>-1</sup> )	$k_{s,sa}$ (Lh <sup>-1</sup> m <sup>-2</sup> ) × 10 <sup>-5</sup>
fast/iron	0.74	1.45 (±5.96)	0.30 (±0.18)	1.2 (±4.1)	6 (±6)
inter./iron	0.74	1.45 (±5.29)	0.37 (±11.51)	0.9 (±3.75)	14 (±11.7)
slow/iron	0.74	1.45 (±8.75)	0.32 (±0.88)	3.2 (±1.70)	15 (±3.1)
fast/Cu-Fe	0.60	2.50 (±0.78)	0.17 (±0.05)	0.6 (±0.19)	7 (±0.8)
inter./Cu-Fe	0.60	2.50 (±0.54)	0.12 (±0.01)	0.3 (±0.05)	3.7 (±4.5)
slow/Cu-Fe	0.60	2.50 (±0.20)	0.13 (±0.06)	1.3 (±0.31)	10 (±2.6)

<sup>a</sup>  $\lambda$  = dispersivity;  $K_d$  = distribution coefficient;  $f$  = fraction of Type-1 sites;  $\alpha$  = first-order kinetic rate sorption constants;  $k_{s,sa}$  = normalized sorbed reaction rate constant constant.



**FIGURE 6.** Iron and Cu-Fe column chloride breakthrough curves through sand. The Cl<sup>-</sup> input pulse was one pore volume for each experiment, and the physical equilibrium advective-dispersive equation was fitted to the curves.

when the retention times within the column increased (Figures 4 and 5). It was also possible that the degradation daughter products were produced but were rapidly reduced to undetectable concentrations in the column effluent.

**Miscible Displacement Model Description.** Gotpager et al. (26) suggested that the slow of TCE degradation with time in batch experiments was possibly caused by mass transfer limitations resulting from corrosion and precipitate buildup on iron surfaces. Furthermore, Cumming et al. (27) demonstrated that iron corrosion and surface precipitates caused physical nonequilibrium transport of bromide in zerovalent metal column experiments. However, Cl<sup>-</sup> breakthrough curves (Figure 6) from the iron and Cu-Fe columns done after the TCE reduction experiments did not display physical nonequilibrium. The physical equilibrium advective-dispersive equation fitted the breakthrough curves well with coefficients of determination ( $r^2$ ; 29) ranging from 0.99 to 0.98. The high  $r^2$  values suggested that there was not a need to consider physical nonequilibrium. Additionally, the largest change in pH was 6.7 to 7.2, which was insufficient to cause carbonate precipitates to build up. The pH may not have changed much because there was a continuous replenishing of water in the influent end of the column.

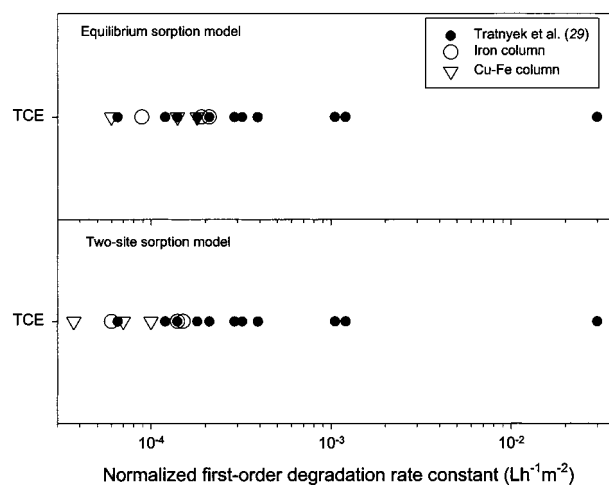


**FIGURE 7.** Figure adapted from Tratnyek et al. ((29) Reprinted by permission of Ground Water Monitoring & Remediation. Copyright 1997.) comparing normalized degradation rates for the iron and Cu-Fe column of this study to previous studies. The normalized degradation rates obtained from curve fits using the equilibrium sorption model (eqs 1a and 1b) and the two-site sorption model (eqs 3a and 3b).

The iron and Cu-Fe column TCE breakthrough data were fitted with the equilibrium sorption model (eqs 1a and 1b) and resulted in good matches between observed and modeled data. The best fit equilibrium sorption model parameters are presented in Table 1. The  $r^2$  values ranged from 0.95 to 0.98 for the iron column and 0.84 to 0.95 for the Cu-Fe column. The optimized  $k_s$  values were used as production coefficients to predict the ethylene breakthrough curves, resulting in  $r^2$  values ranging from 0.92 to 0.97 for the iron column and 0.69 to 0.97 for the Cu-Fe column. The equilibrium sorption model (eqs 1a and 1b) did a good job of fitting the data and produced  $k_s$  values similar to earlier reported values (29) (Figure 7 and Table 1). The column  $\lambda$  values were not significantly different through the range of velocities at a 95% confidence interval (CI) and over a range of  $v$  for a single column  $\lambda$  was expected to be constant (19). In general the  $K_d$  values were not significantly different except at the lower velocities. The most significant difference was the apparent increase of  $k_s$  with an increase in velocity. This may reflect a rate-limiting sorption/diffusion process at the

iron surface. Additionally, the data were fitted with the equilibrium sorption model (eqs 1a and 1b) while holding  $\lambda$  constant for each column. The fixed  $\lambda$  values came from the  $\text{Cl}^-$  breakthrough curves (Figure 6), but good model fits to the data could not be achieved.

The equilibrium sorption model (eqs 1a and 1b) was capable of describing the TCE breakthrough curve data; however, there may have been more complicated sorption. Burris et al. (4) reported Langmuir sorption isotherms of TCE in the presence of iron from batch experiments in addition to sorption onto reactive and nonreactive sorption sites. A two-site sorption model (eqs 3a and 3b, Figure 2) was used to describe the breakthrough curve data, but a linear sorption isotherm was considered instead of Langmuir. The fitted two-site sorption model (eqs 3a and 3b) parameters are presented in Table 1 with their 95% CIs. To increase the uniqueness of the model solution the column  $\lambda$  and  $K_d$  values were held constant (19). The fixed  $\lambda$  values came from the  $\text{Cl}^-$  breakthrough curve experiments (Figure 6;  $\lambda = 0.74$  cm for the iron column and  $\lambda = 0.60$  cm for the Cu-Fe column). Also, the column  $K_d$  values were expected to be constant and were fixed to the best-fitted value from all the TCE breakthrough curves. The iron/TCE Langmuir sorption isotherm from the Burris et al. (4) study was linearized, and the  $K_d$  value was calculated ( $1.47 \text{ L Kg}^{-1}$ ) and found to be very similar to the fitted  $K_d$  value from the two-site sorption model ( $1.45 \text{ L Kg}^{-1}$ , Table 1). The two-site sorption model offered a good description of the breakthrough data and a realistic interpretation of the macroscopic phenomena associated with the breakthrough curves. The TCE breakthrough curve  $r^2$  values ranged from 0.94 to 0.99 for the iron column and 0.97 to 0.98 for the Cu-Fe column. The two-site sorption model predicted the ethylene breakthrough curves better than the equilibrium sorption model (Figure 4 and Figure 5), with  $r^2$  values ranging from 0.97 to 0.99 for the iron column and 0.91 to 0.99 for the Cu-Fe column. The higher  $r^2$  values for the ethylene curves may represent a better physical/chemical description by the two-site sorption model than the equilibrium sorption model; albeit when more fitting parameters are used the model fits are generally better.

The iron and Cu-Fe column  $f$  values did not significantly differ at a 95% CI throughout the range of flow rates. This was expected since the same columns were used for each experiment and the same amount of Type-1 sorption sites should be present for each flow rate. The  $\alpha$  values were not significantly different at a 95% CI, with the exception of the Cu-Fe column where it was highest for the highest  $v$ . Correlations of  $\alpha$  to  $v$  have been noted by other chemical nonequilibrium investigations (30, 31) which may reflect the high velocities that were used for these experiments. The increase of  $\alpha$  with  $v$  may also have reflected some rate-limiting step in the transformation of TCE as it desorbed from reactive sites. This rate-limiting step in the transformation of chlorinated ethylene has been suggested by Burris et al. (32), who speculated that it was caused by the desorption of the solute off of reactive iron sites.

First-order degradation rates normalized to surface area concentration for the two zerovalent metal systems were not significantly different from each other (Figure 7 and Table 1). Nonetheless, lower concentrations of TCE were eluted in the effluent of the Cu-Fe column than the iron column. It has been suggested that higher  $k_s$  values associated with multiple metal systems result from galvanic couples; where one metal preferentially sacrifices electrons or corrodes, further driving the reduction reaction and increasing the rate of TCE degradation (10). It appeared that this was not the case for the miscible-displacement studies because the  $k_s$  values for the iron and Cu-Fe were not significantly different. Rather, it may be that more TCE was removed because there was higher partitioning of TCE into the sorbed

phase. Based on the two-site sorption model, the Cu-Fe  $K_d$  values were generally higher but not significantly different from the iron column values (Table 1).

The normalized first-order degradation rate coefficients from the two transport models were within the range of values measured by previous investigators (29) (Figure 7) but on the lower end. Previous investigators used batch or resident concentration column experiments to estimate their degradation rates and were able to describe the degradation of TCE as a first-order process. However, sorbed concentrations were not measured for the batch and resident concentration column experiments, which may result in overestimated degradation rates of TCE because partitioning and degradation were lumped together. This may explain why the degradation rates for the equilibrium and two-site sorption models were low, because partitioning of TCE from the aqueous solution was considered. Furthermore, the degradation rate for the two-site sorption model would be even smaller because nonequilibrium adsorption-desorption was considered. In fact, earlier reported  $k_s$  values (29) from batch and resident concentration column experiments were more similar to the equilibrium sorption model than the two-site sorption model values (Figure 7). The simpler equilibrium models can describe TCE degradation, but they may be limited because they may not consider other significant processes (i.e., rate-limited sorption). This would be especially important when predicting the tailing or late arrival of TCE leaching from a column.

## Acknowledgments

The authors greatly appreciate the generous grant from the Raymond and Mary Baker Trust. Journal Paper No. J-18801 of the Iowa Agriculture and Home Economic Experiment Station, Ames, Iowa, Project No. 3287, and supported by Hatch Act and State of Iowa Funds.

## Literature Cited

- (1) NAS. *Alternatives for Ground Water Cleanup*; Report of the National Academy of Science Committee of groundwater cleanup alternatives. National Academy Press: Washington, DC, 1994.
- (2) Focht, R. M.; Vogan, J. L.; O'Hannesin, S. F. *Remediation* **1996**, *6*, 81-94.
- (3) Appleton, E. L. *Environ. Sci. Technol.* **1996**, *30*, 536A-539A.
- (4) Burris, D. R.; Campbell, T. J.; Manoranjon, V. S. *Environ. Sci. Technol.* **1995**, *29*, 2850-2855.
- (5) Orth, S. W. M.S. Thesis, University of Waterloo, Ontario, 1992.
- (6) Gillham, R. W.; O'Hannesin, S. F. *Ground Water* **1994**, *32*, 958-967.
- (7) Orth, S. W.; Gillham, R. W. *Environ. Sci. Technol.* **1996**, *30*, 66-71.
- (8) Gillham, R. W.; O'Hannesin, S. F.; Odziemkowski, M. S.; Garcia-Delgado, R. A.; Focht, R. M.; Matulewicz, W. H.; Rhodes, J. E. Enhanced Degradation of VOCs: Laboratory and Pilot-Scale Field Demonstration. 2nd International Containment Technology Conference, Florida State University: Tallahassee, St. Petersburg, FL, 1997; pp 858-863.
- (9) Reinhart, D. R.; Quinn, J. W.; Clausen, C. A.; Geiger, C.; Ruiz, N.; Afioni, G. F. Enhanced Zerovalent Metal Permeable Wall Treatment of Contaminated Groundwater. Second International Containment Technology Conference; Am. Chem. Soc., Div. Environ. Chem., Florida State University: St. Petersburg, FL, 1997; pp 806-812.
- (10) Gavaskar, A.; Sass, B. M.; Drescher, E.; Cumming, L.; Giammar, D.; Gupta, N. Enhancing the Reactivity of Permeable Barrier Media. Designing and Applying Treatment Technologies: Proceedings of the First International Conference on Remediation of Chlorinated and Recalcitrant Compounds, Monterey, CA; Wickramanayake, G. B., Hinchey, R. E., Eds.; Battelle Press: Columbus, OH, 1998; pp 91-96.
- (11) Barry, B. A.; Sposito, G. *Soil Sci. Soc. Am. J.* **1998**, *52*, 3-9.
- (12) Casey, F. X. M.; Ewing, R. P.; Horton, R. *Soil Science*. **2000**, in press.
- (13) Gillham, R. W.; O'Hannesin, S. F. Metal-Catalysed Abiotic Degradation of Halogenated Organic Compounds. IAH Confer-

- ence "Modern Trends in Hydrogeology"; Hamilton, Ontario, Canada, 1992; pp 94–103.
- (14) Brunauer, S.; Emmett, P. H.; Teller, E. *J. Am. Chem. Soc.* **1938**, *60*, 309–319.
- (15) Johnson, T. L.; Scherer, M. M.; Tratnyek P. G. *Environ. Sci. Technol.* **1996**, *30*, 2634–2640.
- (16) Fryzek, T. M.S. Thesis, Iowa State University, Ames, IA, 1998.
- (17) Skopp, J.; Gardner, W. R.; Tyler, E. J. *Soil Sci. Soc. Am. J.* **1981**, *45*, 837–842.
- (18) Toride, N.; Leij, F. J.; van Genuchten, M. Th. *The CXTFIT Code for Estimating Transport Parameter from Laboratory or Field Tracer Experiments. Version 2.0*; Research report no. 137; U.S. Salinity Laboratory, ARS-USDA: Riverside, CA, 1997.
- (19) Bear, J. In *Dynamics of Fluids in Porous Media*; Dover Publications: New York, 1972.
- (20) Šimůnek, J., Šejna, M.; van Genuchten, M. Th. *The HYDRUS-1D Software Package for Simulating the One-Dimensional Movement of Water, Heat, and Multiple Solutes in Variably-Saturated Media*; U.S. Salinity Laboratory, USDA-ARS: Riverside, CA, 1998.
- (21) van Genuchten, M. Th. *Comput. Geosci.* **1985**, *11*, 129–147.
- (22) Selim, H. M.; Davidson, J. M.; Rao, P. S. C. *Soil Sci. Soc. Am. J.* **1977**, *41*, 3–10.
- (23) van Genuchten, M. Th.; Wagenet, R. J. *Soil. Sci. Soc. Am. J.* **1989**, *53*, 1303–1310.
- (24) Sweeney, K. H.; Fischer, J. R. Decomposition of halogenated organic compounds using metallic couples. U.S. Patent # 3, 737, 384. 1973.
- (25) Korte, N.; Muftekin, R.; Grittini, C.; Fernando, Q.; Claussen, J. L.; Liang, L. *ORNL/MMES Research into Remedial Applications of Zerovalent Metals. 2: Bimetallic Enhancements*; American Chemical Society, Division of Environmental Chemistry, 209th ACS National Meeting, Anaheim, CA, 1995; Vol. 35, pp 752–754.
- (26) Gotpagar, J.; Grulke, E.; Tsang, T. Bhattacharyya, D. *Environ. Progress.* **1997**, *16*, 137–143.
- (27) Cumming, L.; Gavaskar, A.; Drescher, E.; Willamson, T.; Drescher, M. Bench-Scale Tracer Tests for Evaluating Hydraulic Performance of Permeable Barrier Media. Proceedings of the First International Conference on Remediation of Chlorinated Recalcitrant Compounds, Monterey, CA; Wickramanayake, G. B., Hinchee, R. E., Eds.; Battelle Press: Columbus, OH, 1998; pp 97–102.
- (28) Snedecor, G. W.; Cochran, W. G. In *Statistical Methods*; 6th ed.; The Iowa State University Press: Ames, IA, 1967; Chapter 7.
- (29) Tratnyek, P. G.; Johnson, T. L.; Scherer, M. M.; Eykholt, G. R. *Ground Water Monit. R.* **1997**, *17*, 108–114.
- (30) Gamedainger, A. P.; Wagenet, R. J.; van Genuchten, M. Th. *Soil Sci. Soc. Am. J.* **1990**, *54*, 957–963.
- (31) Brusseau, M. L. *J. Contam. Hydrol.* **1992**, *5*, 215–234.
- (32) Burris, D. R.; Allen-King, M. A.; Manoranjon, V. S.; Campbell, T. J.; Loraine, G. A.; Deng, B. *J. Environ. Eng.* **1998**, *124*, 1012–1219.

Received for review April 17, 2000. Revised manuscript received August 21, 2000. Accepted August 30, 2000.

ES001185C